Journal of ELECTRONIC MATERIALS, Vol. 48, No. 4, 2019
https://doi.org/10.1007/s11664-019-07020-0

Investigation of a Self-Aligned Cobalt Silicide Process for Ohmic Contacts to Silicon Carbide

MATTIAS EKSTRÖM [1,2] ANDREA FERRARIO [1] and CARL-MIKAEL ZETTERLING [1]

1.—Department of Electronics, School of Electrical Engineering and Computer Science, KTH Royal Institute of Technology, 164 40 Kista, Sweden. 2.—e-mail: mekstr@kth.se

Previous studies showed that cobalt silicide can form ohmic contacts to *p*-type 6H-SiC by directly reacting cobalt with 6H-SiC. Similar results can be achieved on 4H-SiC, given the similarities between the different silicon carbide polytypes. However, previous studies using multilayer deposition of silicon/cobalt on 4H-SiC gave ohmic contacts to *n*-type. In this study, we investigated the cobalt silicide/4H-SiC system to answer two research questions. Can cobalt contacts be self-aligned to contact holes to 4H-SiC? Are the self-aligned contacts ohmic to *n*-type, *p*-type, both or neither? Using x-ray diffraction, it was found that a mixture of silicides (Co_2Si and CoSi) was reliably formed at 800°C using rapid thermal processing. The cobalt silicide mixture becomes ohmic to epitaxially grown *n*-type ($1 \times 10^{19}cm^{-3}$) if annealed at 1000°C, while it shows rectifying properties to epitaxially grown *p*-type ($1 \times 10^{19}cm^{-3}$) for all tested anneal temperatures in the range 800–1000°C. The specific contact resistivity (ρ_C) to *n*-type was 4.3×10^{-4} Ω cm^2. This work opens the possibility to investigate other self-aligned contacts to silicon carbide.

Key words: Cobalt (Co), rapid thermal processing (RTP), self-aligned silicide, silicon carbide (4H-SiC), transfer length method (TLM)

INTRODUCTION

The finding that nickel silicide (Ni_2Si) can be self-aligned to contact holes to silicon carbide (4H-SiC)[1,2] has opened up new research opportunities. An example of such a study was the finding that the self-aligned Ni_2Si can be turned from rectifying to ohmic to *p*-type 4H-SiC by alloying it with aluminum at relatively low temperatures.[3] A comparison between self-aligned nickel silicide and lift-off process for power devices was recently presented by Sledziewski at the conference of silicon carbide and related materials (ECSCRM 2018). Nickel-based contact processes give good ohmic contacts to *n*-type 4H-SiC,[2,4,5] but often gives rectifying contacts to *p*-type, with some notable exceptions.[6–8] As such, there is currently missing a single-metal process for self-aligned ohmic contacts to *p*-type. It is known from the mature silicon technology that, in addition to nickel silicide,[9–11] titanium-,[10–13] cobalt-[10,11,13] and platinum-silicide[14] can be self-aligned. Given the similarities between silicon and 4H-SiC, some or all of the silicides that can be self-aligned to silicon can be self-aligned to SiC. Thus, it is of interest to investigate the other silicide-forming systems.

Lundberg and Östling[15] showed that cobalt silicides ($CoSi_x$) form ohmic contacts to *p*-type 6H-SiC. The SiC polytypes have similarities and differences. The bandgap energy is similar between the two polytypes (3.02 eV and 3.26 eV at 300 K for 6H and 4H, respectively.[16]) The energy difference between vacuum energy (E_0) and valence band edge (E_V) is approximately the same between different polytypes ($E_0 - E_V \sim 7.1$ eV).[17–19] If the $CoSi_x$/6H-SiC contact that Lundberg and Östling found was a Schottky–Mott-like ohmic contact, it would be

(Received October 29, 2018; accepted January 29, 2019; published online February 12, 2019)

reasonable to assume that it would also be ohmic to 4H, albeit with a slightly higher Schottky barrier. As such, self-aligned $CoSi_x$ was considered as a candidate for low resistance ohmic contacts to *p*-type 4H-SiC. However, it is known that contacts to 4H-SiC are not perfect Schottky–Mott contacts. 4H-SiC contacts have at least partial Fermi-level pinning,[20] and as such it can be inferred that similar valence band energy does not guarantee similar hole Schottky barrier height. The close chemical similarity between cobalt (atomic number 27) and nickel (atomic number 28) could imply similar characteristics. As such, the $CoSi_x$/4H-SiC system could instead give low resistance ohmic contacts to *n*-type 4H-SiC, just like the Ni_2Si/4H-SiC system. $CoSi_2$/4H-SiC, formed by multilayer deposition of silicon and cobalt, has been previously studied and been shown to provide low resistance ohmic contact to *n*-type 4H-SiC,[21–23] and the result to *p*-type 4H-SiC is unclear.[24]

We investigated the $CoSi_x$/4H-SiC system to answer the following two research questions[25]:

1. Can $CoSi_x$ be self-aligned to 4H-SiC?
2. Does self-aligned $CoSi_x$ form ohmic contacts to *n*-type, *p*-type, both or neither?

In this work, we present the results and conclusions of our investigations. The difference from previous contact studies to 4H-SiC is that only cobalt is deposited instead of the silicon/cobalt multilayer stacks.[21–23] Moreover, interface reactions between cobalt and 4H-SiC are studied using rapid thermal processing (RTP) to anneal cobalt/4H-SiC instead of furnace annealing cobalt/6H-SiC.[26,27]

The annealing temperature range was limited in this study up to 1000°C. It was considered that any contact process requiring higher annealing temperatures than 1000°C would not be competitive with already established contact processes.[2,3,21–23,28–30] Higher anneal temperatures could potentially degrade other device related properties, like the silicon dioxide (SiO_2)/4H-SiC interface of metal oxide semiconductor field-effect transistors (MOSFETs).

EXPERIMENTAL DETAILS

Three different sets of 4H-SiC samples (10 mm × 10 mm pieces) were prepared. The first set was used for x-ray diffraction (XRD) characterization. These pieces came from a 100 mm 4° off-axis cut *n*-type substrate wafer (SiCrystal, 0.0175 Ω cm, corresponding to $\sim 3 \times 10^{18}\,cm^{-3}$ nitrogen doping) with (0001) orientation. Although there may be subtle differences in silicide formation between substrate pieces and epitaxy pieces (through differences in doping and mechanical properties), we assume that the substrate pieces are a good model for silicide formation on epitaxy.

The second set was used to determine the specific contact resistivity to both *n*-type and *p*-type 4H-SiC. The epitaxy was grown by Norstel, and was, from top to bottom: 1 μm *n*-type of $10^{19}\,cm^{-3}$ doping concentration and 1 μm *p*-type of $10^{18}\,cm^{-3}$ doping concentration. The epitaxy was grown on a 100 mm 4° off-axis cut *n*-type substrate wafer. The *p*-type layer provides a *pn*-junction isolation for the top *n*-type layer, and the *p*-type layer is isolated from the *n*-type substrate by the formed *pn*-junction. These doping levels correspond to those used in our in-house bipolar junction transistor (BJT) technology, and as such it would be an interesting finding if the cobalt contacts would provide low resistance ohmic contacts to both *n*-type and *p*-type at the same time.

The third and final set had highly doped *p*-type epitaxy. The epitaxy was grown by Norstel and was, from top to bottom: 200 nm *p*-type of $10^{19}\,cm^{-3}$ doping concentration, 800 nm *n*-type $10^{16}\,cm^{-3}$ doping concentration, and 1 μm *p*-type of $5 \times 10^{18}\,cm^{-3}$ doping concentration. The epitaxy was grown on a 100 mm 4° off-axis cut *n*-type substrate wafer. The different *pn*-junctions provide isolation between the different layers. This third set has a higher *p*-type doping than the second set, which should enhance field emission (FE) by having a narrower depletion region. If the $CoSi_x$ would form low resistance ohmic contacts to *p*-type, it was expected that this third set would have lower contact resistance to *p*-type than the second set.

The samples with epitaxy (sets 2 and 3) were prepared to have transfer length method (TLM) structures by forming TLM mesas. These mesas limit the current flow to laminar flow between contacts. By limiting the current flow, the accuracy of the extraction of the specific contact resistivity is improved.[31] The mesas were patterned by standard optical lithography and were dry etched by magnetically enhanced reactive ion etching (MERIE). The second set was etched twice in order to provide mesa isolation for both *n*-type and *p*-type, whereas the third set was etched once to provide isolation for the top *p*-type layer. Since dry etching induces surface damage, the wafers underwent sacrificial oxidation, where the surface is oxidized and removed by stripping the grown oxide with hydrofluoric acid. At this point, all three wafers could be diced into pieces for further processing.

All three sets of samples were cleaned in Piranha solution (H_2SO_4 mixed with H_2O_2) for 5 min to remove any organic material, followed by diluted HF (dHF) for 5 min to remove any chemical SiO_2.

To enable the self-aligned process, a 50 nm SiO_2 film was deposited by atomic layer deposition (ALD) at 350°C with ozone (O_3) and a commercial precursor (AP-LTO-330) on the epi-layer samples. This ALD-SiO_2 film has a very low density of pinholes and provides excellent isolation to prevent unwanted Co/4H-SiC reactions. The SiO_2 film also provides some surface passivation. In preparation

for a future dHF-dip, the SiO_2 was hardened by annealing it in a RTP tool (a Mattson 100 RTP system) for 30 s at 1000°C in N_2 ambient. Contact holes were patterned by standard optical lithography and opened with a conventional polymer-forming fluorine-based ($Ar/CF_4/CHF_3$) MERIE process that etches SiO_2 selectively to 4H-SiC. The resist was stripped by chemical remover and post-cleaned with solvents. To ensure complete removal of organics, the samples were further cleaned by O_2-plasma and 5 min Piranha.

Before cobalt deposition, all three sets were cleaned by dipping the samples in dHF (10:1 H_2O : 5% HF *v/v*) for 10 s followed by thorough rinsing and drying. Cobalt was deposited in a Lesker CMS-18 magnetron sputter operated in direct-current magnetron sputtering (DCMS) mode with an average discharge power of 130 W. The sputtering gas was argon at a pressure of 1.1 Pa and a mass flow of 80 sccm. At these conditions, the deposition rate was 2.33 nm/min. No intentional heating was used, nor was backsputtering performed to pre-clean the samples. 10 nm of cobalt was deposited on the epi-samples and 40 nm of cobalt was deposited on the XRD samples. It was considered that the direct cobalt/4H-SiC reaction would release large amount of carbon that could be detrimental for the contact. The thin film thickness of 10 nm is primarily motivated by the need to reduce the amount of released carbon. Cobalt, like nickel and platinum, does not form carbides when directly reacting with 4H-SiC. The released carbon forms precipitates inside of the silicide film, or graphite if the annealing temperature is sufficiently high.[27] One of the motivations for the multilayer silicon/cobalt depositions was to reduce the amount of released carbon.[15,21–23] The 40 nm cobalt was motivated by the need to have strong XRD signals. A few substrate pieces (set 1) had only 10 nm cobalt, which was used in XRD and scanning electron microscopy (SEM).

The XRD samples were annealed in the temperature range 600–850°C using the RTP system for 30–240 s in N_2 ambient. The samples were annealed inside of a graphite box that was heated by lamps. The high thermal mass of the graphite box prevents investigating anneal times shorter than 30 s, and 240 s was the longest time allowed without damaging the RTP system. The temperature was controlled in a feedback loop by an optical pyrometer that measures the temperature of the graphite box. The pyrometer was calibrated by thermocouple measurement of a silicon wafer inside of the graphite box. The oxygen content inside of the chamber was monitored by an O_2-meter. The chamber was purged with nitrogen until the oxygen content was below one part per million (*v/v*) before ramping up to process temperature. The error in steady-state temperature is a few degrees celsius (< 10°C) for this setup. It was found that $CoSi_x$-phase could be formed reliably at 800°C from the XRD results (see "Structural Characterization" Section), which was selected as the first-step anneal (FSA) of the self-aligned process.

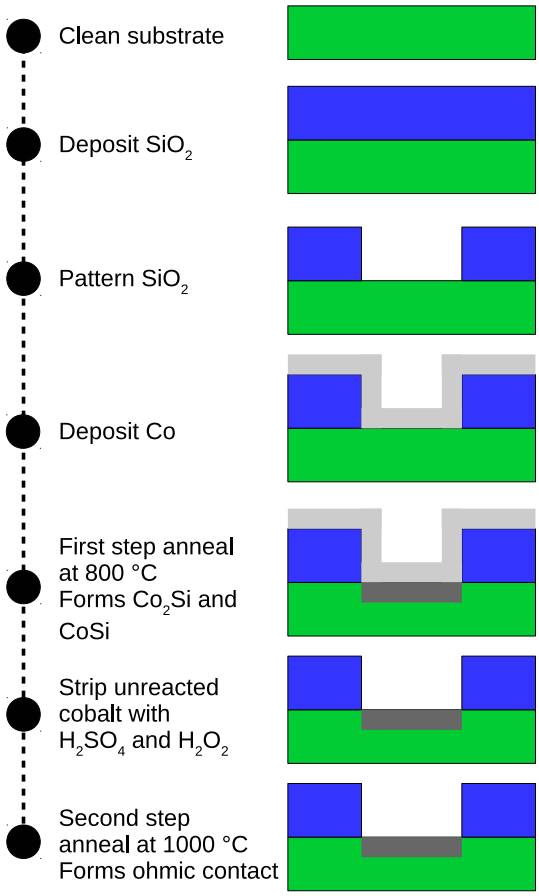

Fig. 1. Simplified process flow for ohmic contact formation to *n*-type SiC using cobalt silicide.

The unreacted cobalt was stripped by Piranha solution after the FSA. The samples were annealed a second time at temperatures varying from 850°C to 1000°C in steps of 50°C, with the time (60 s) and ambient (N_2) remaining the same amongst the samples. One sample from each of the two epi-layer sets was not subjected to the second-step anneal (SSA) to check if the FSA was sufficient to form ohmic contacts.

The samples were further processed by depositing metallization (TiW and aluminum) to allow for measurement pads. The metallization was patterned by standard optical lithography and etched by a combination of reactive ion etching (RIE) and wet etching.

A simplified self-aligned process flow is shown in Fig. 1. The TLM structures (without TiW/Al metallization) are illustrated in Fig. 2.

The XRD characterization was performed by θ–2θ scan using a PANalytical Empyrean with Cu $K_{\alpha,1}$ radiation. The incident x-ray beam optics included a nickel filter (removes Cu K_β radiation), a hybrid 2 × Ge(220) monochromator [an x-ray mirror and two

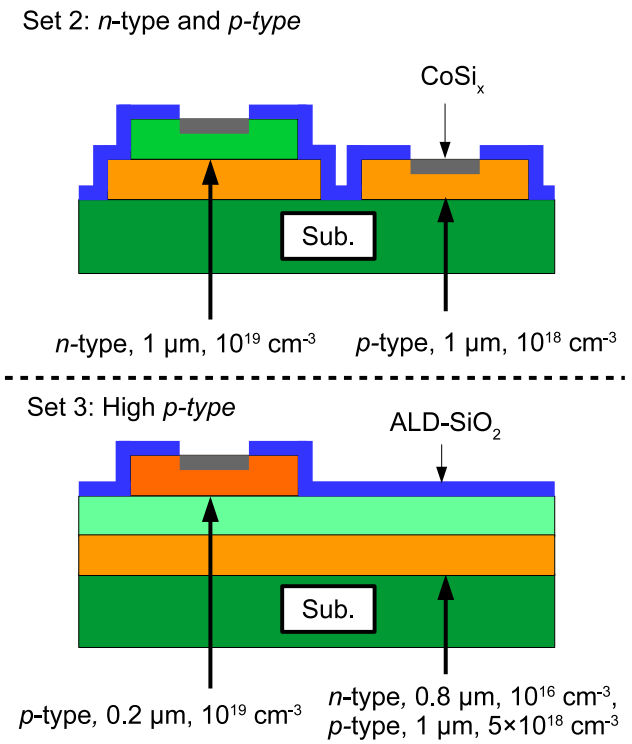

Fig. 2. Simplified cross-section view of the TLM structures used in this study (not drawn to scale). Set 2 samples had both *n*-type and *p*-type TLM structures, whereas set 3 had high *p*-type doping. This drawing is without top-level metallization.

Ge(220) crystals that suppress the Cu $K_{\alpha,2}$ radiation], a 0.125° divergence slit, a 0.5° anti-scatter slit, a Soller slits assembly and a beam-mask. The diffracted beam path consisted of fixed anti-scatter slits and another Soller slits assembly. The samples were mounted on a reflection-transmission spinner. The surface morphology was investigated by SEM using a Zeiss Ultra 55 with with an in-lens detector that images the topography and an integrated energy-dispersive x-ray spectroscopy (EDS) system. SEM images were captured with an electron beam energy of 2 keV, whereas the x-ray signal for EDS analysis was excited with an electron beam energy of 10 keV. The electrical characterization was performed with a Cascade 11000 probestation connected to a Keithley 4200-SCS. The samples were inside of a microchamber that shields the samples from ambient light and electromagnetic interference. Four-probe measurement (Kelvin measurement) was used to eliminate the resistance of the cables.

RESULTS AND DISCUSSION

Structural Characterization

The measured XRD spectra of substrate samples with 40 nm cobalt are shown in Fig. 3. The as-deposited cobalt films do not exhibit any XRD peak that corresponds to crystalline cobalt. A possible explanation is that the film is nanocrystalline and the crystallinity cannot detected in θ–2θ scans,

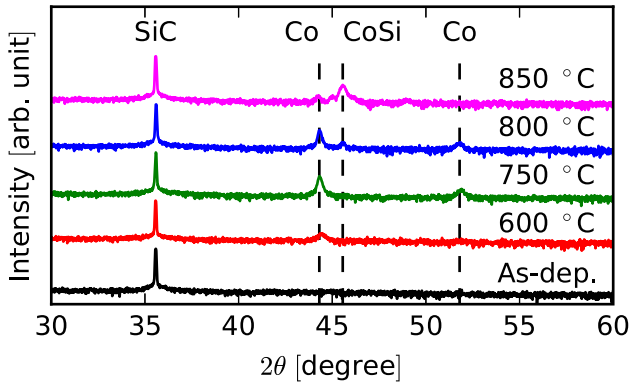

Fig. 3. XRD spectra of $CoSi_x$/SiC. The as-deposited film does not show enough large-grain crystallinity to be detected by θ–2θ scans. The cobalt film crystallizes at 600°C. The cobalt silicides form at 800°C and above by RTP, 60 s. The initial cobalt thickness was 40 nm for all samples.

although it may be detected by grazing-incidence x-ray diffraction (GIXRD).[32] The cobalt signal emerges after annealing the film at 600°C at $2\theta = 44.3°$, correspondig to cubic (111), and around $2\theta = 52°$, corresponding to cubic (200).[26] The film likely forms large polycrystalline grains at this anneal temperature that can be detected by the θ–2θ scan. Annealing at 750°C increases the cobalt signal. Both Co_2Si at $2\theta = 44.3°$, corresponding to (021), and CoSi at $2\theta = 45.5°$, corresponding to (210), are found at 800°C. This temperature is somewhat lower than the lowest tested temperature in Ref. 27 (850°C), but higher than the formation temperature found by Ref. 26. It should be stressed that polycrystalline 6H-SiC and anneals longer than 10 min was used in the work of Ref. 26 to find Co_2Si at 650°C. It is surprising to find both Co_2Si and CoSi co-existing at this narrow anneal condition. Given the auricupride-rule, the most mobile species determines the first phase. As such, it is commonly observed that the first phase is the metal-rich silicide (X_2Si, X=Co, Ni, Ti, Pt).[11,26,27] Given the finding that Co_2Si may form at 650°C after long anneals, the process bottleneck appears to be the nucleation of Co_2Si. The thermally activated probability per unit time of nucleating the silicide increases with increasing temperature, and as such Co_2Si may form within 60 s at 800°C with very high probability but with very low probability at 750°C. CoSi may also form at this temperature, but requires that Co_2Si forms first. However, to verify these assumptions would require detailed investigation at the kinetics of formation of the cobalt/4H-SiC system which was outside the scope of this study. Higher annealing temperatures transform the Co/Co_2Si to CoSi, as evident by the decreased signal at $2\theta = 44.3°$ [cubic cobalt (200) and Co_2Si (021)] and increased signal at $2\theta = 45.5°$ [CoSi (210)].

To verify that the $CoSi_x$ had formed at 800°C, the sample was submerged in Piranha solution to etch cobalt selectively to the silicides. The sample was re-measured and it was found that the signal at $2\theta =$

44.3° decreased [reduced cubic cobalt (200) signal] but did not disappear [Co_2Si (021) signal remained]. It appears that Co, Co_2Si and CoSi coexist at 800°C. This has been observed in previous studies on 6H-SiC[26] and in silicon technology.[13]

A difference from the nickel/4H-SiC system is that both Co_2Si and CoSi are formed, whereas Ni_2Si is thermally stable for typical process temperatures. The co-existence of multiple phases can be both beneficial and detrimental. The use of phase-segregation in Pt:Ti/4H-SiC system allows for ohmic contacts to both *p*-type and *n*-type by having locally varying Schottky barrier height,[28] and as such having multiple $CoSi_x$ phases could give simultaneous contacts. However, if only one phase gives ohmic contacts to one of the types, then the contact would exhibit high resistance. As such, it is important to have control of which phase is present. Phase control appears difficult at low temperatures ($\sim$ 800°C), due to Co, Co_2Si and CoSi coexisting. Phase control is possible by having high temperature anneal, since the final silicide phase is CoSi in the Co/4H-SiC system.

The time required to form the silicide was investigated by varying the anneal time, 30 s, 60 s and 240 s. The $CoSi_x$-signals are weak but present at 30 s, and there was no significant difference between 60 s and 240 s. As such, it was determined that annealing at 800°C for 60 s was the most suitable FSA condition. This temperature is 200°C higher than that of the FSA of the self-aligned nickel silicide contacts to 4H-SiC for the same annealing conditions (RTP process) and time.[2] It is possible that the nucleation can be enhanced, and thus lower the temperature, by having a cleaner interface during the deposition. *In situ* clean by backsputtering and thermal desorption of moisture by in-situ heat treatment prior to deposition are two possible improvements. Reducing the FSA temperature would greatly improve the process, as it would inhibit the defect formation mechanisms that are typical of self-aligned silicide processes. While direct reaction of cobalt with SiO_2 at 800°C is thermodynamically unfavorable,[33] cobalt can react with SiO_2 at 800°C in the presence of oxygen contamination.[34] To avoid this possibility, the FSA temperature should be kept under 700°C.[10] In the absence of reaction, the cobalt could conceivably diffuse through the SiO_2 through defects or pinholes (depending on the quality of SiO_2) and react with the underlying 4H-SiC. Of more concern is the commonly observed silicon-diffusion causing bridging-fault, wherein silicon atoms, which are the dominant diffusers in forming CoSi, diffuse from the silicon source (in this case 4H-SiC) through the CoSi and reacts with the cobalt lying on the SiO_2 between contacts. There, it can form a silicide that bridges between contacts and cause short-circuit.[10,11,13] Reducing the temperature would reduce the thermally activated diffusion of both cobalt through SiO_2 and silicon through CoSi.[13] Unless future studies find a way to reduce this FSA temperature, the cobalt self-aligned process will result in poor yield due to the generation of a high number of defects.

The surface morphology was studied by SEM and chemically by EDS. The samples that were imaged were substrate pieces with varying initial cobalt thickness (both 10 nm and 40 nm). The 10 nm cobalt sample is patchy and non-uniform after the FSA but before stripping the cobalt (Fig. 4). EDS detects that the surface is covered with cobalt, as expected. Samples with stripped remaining cobalt are different for different initial cobalt thicknesses. The thin 10 nm cobalt sample have hexagonal crystallites on the surface, as seen in Fig. 5a. The hexagonal crystallites have a much higher Co L_α signal than the surrounding (darker) area, and as such these crystallites are likely the remaining $CoSi_x$. However, the thick 40 nm cobalt sample give a very different surface. The cobalt has reacted with 4H-SiC, as seen by the blistered surface in Fig. 5b. The blistered surface is not $CoSi_x$, according to EDS. The $CoSi_x$ itself is a dendric-like structure. As such, the $CoSi_x$ appears to break when the initial thickness is 40 nm. The $CoSi_x$ does not form a continuous film in both cases. Similar results can be found in silicon technology. Thinner films are dominated by the interface energy and allows better silicidation growth, whereas thicker films can break because they are unable to handle the strain at the silicide/silicon.[35] However, thin films agglomerate (form islands) easier than thick films.[13] As such, the choice of initial cobalt thickness turned out to be non-trivial. Future studies could investigate the thickness dependence.

Electrical Characterization

For the purpose of determining if the contacts were ohmic or not, a pair of adjacent TLM contacts were measured by sweeping the current, from $-10\,\mu$A to $10\,\mu$A in steps of $1\,\mu$A, and measuring the voltage drop. An ohmic contact produces a

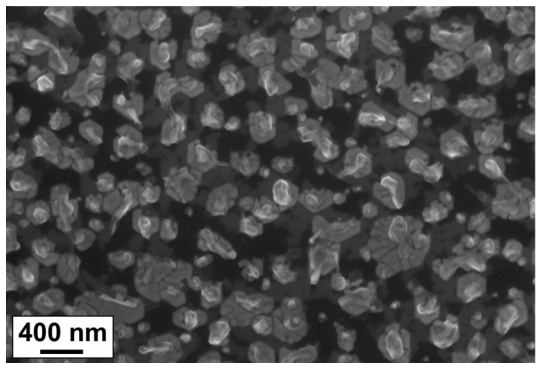

Fig. 4. SEM image of cobalt silicide mixture, formed at 800°C, RTP and 60 s from 10 nm cobalt/4H-SiC. The sample has not been stripped of unreacted cobalt. The surface is patchy and non-uniform.

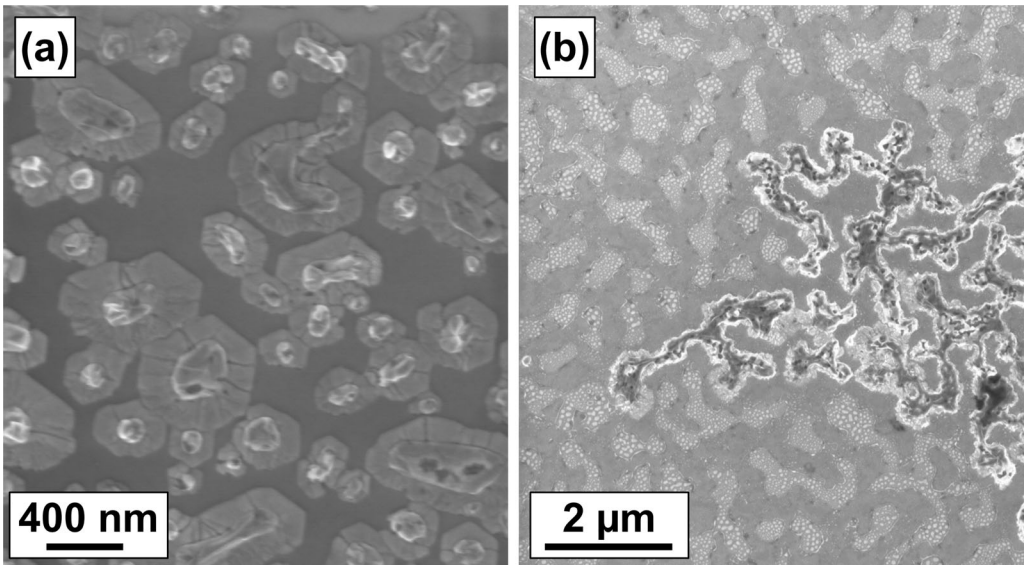

Fig. 5. SEM image of cobalt silicide, formed at 800°C, RTP and 60 s from cobalt/4H-SiC. The unreacted cobalt has been stripped. (a) The sample had 10 nm initial cobalt thickness. The $CoSi_x$ forms hexagonal islands by agglomeration. Since $CoSi_x$ is cubic/orthorhombic, it appears to grow textured partially in the {111} direction. (b) The sample had 40 nm initial cobalt thickness. The $CoSi_x$ film has broken and forms dendric-like structures, as seen in the center right-hand side part of the figure. The surrounding 4H-SiC surface appears blistered, which indicates the the cobalt had a reaction with the 4H-SiC before breaking. Note that the magnification is higher in (a) than (b).

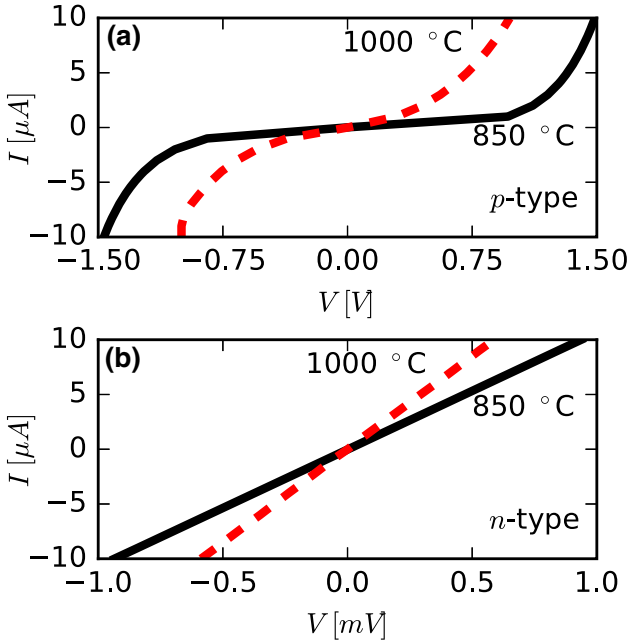

Fig. 6. $I-V$ curves from measured contact pairs. (a) shows contacts to *p*-type 4H-SiC and (b) shows contacts to *n*-type 4H-SiC, both with a doping concentration of 10^{19}cm^{-3}. The contacts to *p*-type 4H-SiC show 'S' curve and are non-ohmic. The contacts to *n*-type 4H-SiC are ohmic after annealing at 850°C and the resistance decreases with higher anneal temperature. The solid lines are for contacts annealed at 850°C and the dashed lines for contacts annealed at 1000°C. Note that the voltage scale differs for *n*-type and *p*-type, while the same current scale is used.

straight line in an $I-V$ plot, whereas non-ohmic contacts produce an 'S'-curve. A selected few $I-V$ curves are shown in Fig. 6.

All measured contact pairs on *p*-type, regardless of the doping level used, showed "S"-curve (as seen in Fig. 6a), indicating that the contacts were very poor. The partially rectifying behaviour also demonstrates that there are no metallic short-circuits between the contacts, which would be caused by cobalt/4H-SiC reaction under the SiO_2 or by bridging between the contacts. $CoSi_x$ formed only in the open contact areas, otherwise there would have been metallic short-circuits. The resistance of the *p*-type contacts decreased by higher SSA temperature, but it was still partially rectifying even at 1000°C. Even if the contacts become ohmic at a higher annealing temperature, the process is unlikely to be competitive with already established contact processes.[3,28–30] As such, it was found that the self-aligned $CoSi_x$ is a poor candidate for low resistance ohmic contacts to *p*-type 4H-SiC. It is interesting to compare the result to that achieved by Lundberg and Östling.[15] They achieved ohmic contacts (about 10^{-3} Ω cm^2) by annealing 120 nm Co/6H-SiC (2×10^{19} cm^{-3}, epitaxy) at 900°C for 2 h in a vacuum furnace. Five parameters are different between these experiments: doping concentration, thickness, time, polytype and annealing system. The twice higher doping gives 1.4× narrower depletion width, which may be sufficient to enable tunneling. However, contacts to 4H-SiC are almost always determined by thermionic field emission (TFE) and not FE, and as such this small doping concentration difference may not be enough to change a rectifying contact to an ohmic contact. The thickness may play a role if the amount of released carbon is important—otherwise the interface alone should determine the contact properties. Since the process

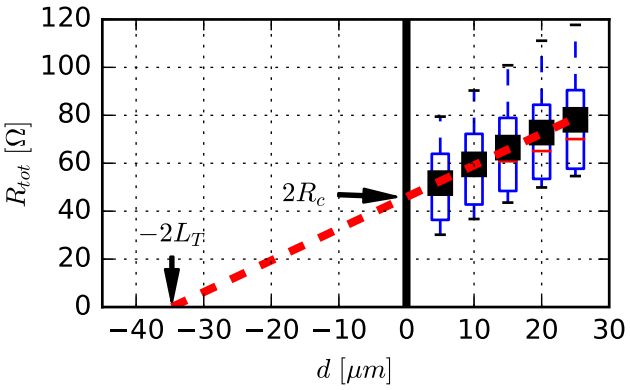

Fig. 7. TLM boxplot of cobalt silicide contacts to *n*-type 4H-SiC, annealed at 1000°C. The whiskers show the range of total resistance (R_{tot}) values of the four measured TLM structures. The contact resistance ($2R_c$) is given by the intercept at zero separation distance (d). The transfer length ($2L_T$) is given by the intercept at zero resistance. The separation distance of the contacts were 5 μm, 10 μm, 15 μm, 20 μm and 25 μm, and the width was 100 μm.

bottleneck is the silicide nucleation, the time and temperature might not be the most important parameters for a Schottky–Mott contact—a higher temperature together with a shorter time can produce the same silicide as a lower temperature for a longer anneal time. What might be important is to have one $CoSi_x$-phase instead of having a mixture, which would be achieved by a long anneal. The same silicide should, ideally, give the same work function. As argued in the introduction, while there are differences between the polytype, the valence bands are similar, and as such the Schottky barrier should be similar between the different polytypes for the same metal work function. It is possible that the higher resistance observed for our contacts is entirely due to the small difference in Schottky barrier, but it is also possible that these contacts are not Schottky–Mott contacts, but some other intermediate contacts, like metal-induced gap states (MIGS) contact.

Ohmic contact behaviour was found for all contacts to *n*-type 4H-SiC annealed at 850°C and higher, as seen in Fig. 6b. Higher SSA temperatures give lower contact resistance. However, the contacts produced a very high resistance with high variability up to 1000°C anneal temperature. Because of this variability, it was not possible to fit the data to the TLM-model—the variation was larger than the resistance difference due to the *n*-type sheet resistance. Only the sample annealed at 1000°C gave low enough contact resistance with low variability to fit the data to the TLM-model, as shown in Fig. 7. The extracted specific contact resistivity of the 1000°C sample was, averaged over four structures, 4.3×10^{-4} Ω cm^2 (sample standard deviation was 2.7×10^{-4} Ω cm^2) at room temperature. Compared to the $CoSi_2$/4H-SiC contacts, produced by multilayer silicon/cobalt deposition, the result is unfavourable. Cho et al. achieved ρ_C of 1.8×10^{-6} Ω cm^2 by annealing at 800°C for 2 min.[21,22] Smedfors et al. achieved ρ_C of 3.8×10^{-5} Ω cm^2 by annealing at 950°C for 1 min.[23] It is stressed that the doping of our samples are nominally identical to those of Smedfors et al. While the multilayer deposition process is more complex, as it requires both lift-off and capability to deposit silicon and cobalt at the same time unlike the self-aligned and direct reaction between Co/4H-SiC, it achieves better results. A major difference between previous contacts and these contacts is that the multilayer contacts produce silicon-rich $CoSi_2$ as final phase, whereas our approach gives metal-rich phases (Co_2Si and CoSi). It might be inferred that $CoSi_2$ results in better contacts to *n*-type 4H-SiC than the other silicide phases. $CoSi_2$ gives a smaller electron Schottky barrier height to silicon than CoSi,[11] which might be same case for 4H-SiC. There could be other reasons why the multilayer approach gives lower contact resistivity. The multilayer approach minimizes the reaction with 4H-SiC, which minimizes surface roughening and carbon release, which in turn could give lower contact resistivity. Another observation is that the microstructure of our $CoSi_x$ has agglomerated into islands and is not a continuous film, whereas there is a continuous film in both of the work of Cho et al.[21] and Smedfors et al.[23] (although in the latter case voids were seen in SEM). The crystallites would form point-contacts and behave differently from the continous film case seen in the previous studies.

Compared to the already established self-aligned nickel silicide process, the result is also unfavourable. Elahipanah et al.[2] achieved ρ_C of 5×10^{-6} Ω cm^2 by annealing at 950°C for 1 min as the SSA.

The sheet resistance showed considerable spread in values, ranging from 101 Ω/ to 194 Ω/. This may influence the contact result if the doping variation is the primary cause of sheet resistance variation. This small dataset does not show correlation (the *p*-value of the null-hypothesis, no correlation, is 60%), and as such we cannot show that the doping is causing the specific contact resistivity variation. However, the average sheet resistance (132 Ω/) is within the expected order of magnitude.[23]

CONCLUSIONS

This study investigated if cobalt silicide could be self-aligned to contact holes to 4H-SiC and give ohmic contacts to *n*-type, *p*-type, both or neither. We successfully found that self-aligned cobalt silicide forms ohmic contacts to *n*-type by first annealing at 800°C, stripping the remaining cobalt, followed by a second anneal at 1000°C. While successful, the performance of this contact is inferior to the already established self-aligned nickel silicide contact process. Both the temperature formation and specific contact resistivity is higher for the cobalt silicide than that of the nickel silicide process. The

presented process could possibly be improved by *In situ* cleaning during sputtering and by using different film thicknesses, but this remains to be investigated.

With this study, we have shown that not only nickel silicide can be self-aligned to 4H-SiC, and as such future work could be to investigate if the other two silicide forming systems, Ti/4H-SiC and Pt/4H-SiC, can form self-aligned ohmic contacts. It is possible that the combinations Ni:Pt/4H-SiC and Pt:Ti/4H-SiC could also be self-aligned.

ACKNOWLEDGMENTS

Thanks goes to Tomas Kubart for assisting in the cobalt deposition. Thanks goes to Gunnar Malm, who provided much appreciated feedback on the manuscript. The authors thank the Knut and Alice Wallenberg Foundation for funding this research as a part of the Working on Venus project.

OPEN ACCESS

REFERENCES

1. A. Stavrinidis, G. Konstantinidis, K. Vamvoukakis, and K. Zekentes, *Mater. Sci. Forum* (2017). https://doi.org/10.4028/www.scientific.net/MSF.897.407.
2. H. Elahipanah, A. Asadollahi, M. Ekström, A. Salemi, C.M. Zetterling, and M. Östling, *ECS J. Solid State Sci. Technol.* (2017). https://doi.org/10.1149/2.0041705jss.
3. M. Ekström, S. Hou, H. Elahipanah, A. Salemi, M. Östling, and C.M. Zetterling, *Mater. Sci. Forum* (2018). https://doi.org/10.4028/www.scientific.net/MSF.924.389.
4. S.Y. Jiang, X.Y. Li, and Z.Z. Chen, *IEEE Trans Electron Devices* (2018). https://doi.org/10.1109/TED.2017.2784098.
5. V.K. Sundaramoorthy, R.A. Minamisawa, L. Kranz, L. Knoll, and G. Alfieri, *Mater. Sci. Forum* (2018). https://doi.org/10.4028/www.scientific.net/MSF.924.413.
6. N. Kiritani, M. Hoshi, S. Tanimoto, K. Adachi, S.I. Nishizawa, T. Yatsuo, H. Okushi, and K. Arai, *Mater. Sci. Forum* (2003). https://doi.org/10.4028/www.scientific.net/MSF.433-436.669.
7. K.C. Kragh-Buetow, R.S. Okojie, D. Lukco, and S.E. Mohney, *Semicond. Sci. Technol.* (2015). https://doi.org/10.1088/0268-1242/30/10/105019.
8. H. Shimizu, A. Shima, Y. Shimamoto, and N. Iwamuro, *Jpn. J. Appl. Phys.* (2017). https://doi.org/10.7567/JJAP.56.04CR15.
9. D.X. Xu, S.R. Das, C.J. Peters, and L.E. Erickson, *Thin Solid Films* (1998). https://doi.org/10.1016/S0040-6090(98)00547-1.
10. J.P. Gambino, E.G. Colgan, and *Mater. Chem. Phys.* (1998). https://doi.org/10.1016/S0254-0584(98)80014-X.
11. S.L. Zhang, and M. Östling, *Crit. Rev. Solid State Mater. Sci.* (2003). https://doi.org/10.1080/10408430390802431.
12. C.K. Lau, Y.C. See, D.B. Scott, J.M. Bridges, S.M. Perna, and R.D. Davies, *IEEE International Electron Devices Meeting (IEDM)* (1982), pp. 714–717.
13. K. Maex, *Mater. Sci. Eng. R* (1993). https://doi.org/10.1016/0927-796X(93)90001-J.
14. Z. Zhang, S.L. Zhang, M. Östling, and J. Lu, *Appl. Phys. Lett.* (2006). https://doi.org/10.1063/1.2194313.
15. N. Lundberg, and M. Östling, *Solid-State Electron.* (1996). https://doi.org/10.1016/0038-1101(96)00071-8.
16. T. Kimoto and J.A. Cooper, *Fundamentals of Silicon Carbide Technology* (Wiley, Singapore, 2014), p. 33.
17. A.O. Evwaraye, S.R. Smith, and W.C. Mitchel, *Appl. Phys. Lett.* (1995). https://doi.org/10.1063/1.115233.
18. V.V. Afanas'ev, M. Bassler, G. Pensl, M.J. Schulz, and E. Stein von Kamienski, *J. Appl. Phys.* (1996). https://doi.org/10.1063/1.361254.
19. G. Pasold, F. Albrecht, J. Grillenberger, U. Grossner, C. Hülsen, W. Witthuhn, and R. Sielemann, *J. Appl. Phys.* (2003). https://doi.org/10.1063/1.1539539.
20. S.K. Lee, C.M. Zetterling, and M. Östling, *J. Electron. Mater.* (2001). https://doi.org/10.1007/s11664-001-0023-1.
21. N.I. Cho, K.H. Jung, and Y. Choi, *Semicond. Sci. Technol.* (2004). https://doi.org/10.1088/0268-1242/19/3/003.
22. S.J. Yang, C.K. Kim, I.H. Noh, S.W. Jang, K.H. Jung, and N.I. Cho, *Diam. Relat. Mater.* (2004). https://doi.org/10.1016/j.diamond.2003.10.067.
23. K. Smedfors, C.M. Zetterling, and M. Östling, *Mater. Sci. Forum* (2015). https://doi.org/10.4028/www.scientific.net/MSF.821-823.440.
24. K. Smedfors, Ohmic Contacts for High Temperature Integrated Circuits in Silicon Carbide (KTH Royal Institute of Technology, Stockholm, 2014).
25. A. Ferrario, Processing and characterization of self-aligned Ni/Al and Co ohmic contacts to 4H-SiC (KTH Royal Institute of Technology, Stockholm, 2018).
26. T. Fujimura, and S.I. Tanaka, *J. Mater. Sci.* (1999). https://doi.org/10.1023/A:1004750016287.
27. C.S. Lim, J.S. Ha, J.H. Ryu, K.H. Auh, I.T. Bae, M. Ishimaru, and Y. Hirotsu, *Mater. Trans.* (2002). https://doi.org/10.2320/matertrans.43.1225.
28. R.S. Okojie, and D. Lukco, *J. Appl. Phys.* (2016). https://doi.org/10.1063/1.4968572.
29. M. Vivona, G. Greco, C. Bongiorno, S. Di Franco, R. Lo Nigro, S. Scalese, S. Rascunà, M. Saggio, and F. Roccaforte, *Mater. Sci. Forum* (2018). https://doi.org/10.4028/www.scientific.net/MSF.924.377.
30. R. Nipoti, M. Puzzanghera, M. Canino, G. Sozzi, and P. Fedeli, *Mater. Sci. Forum* (2018). https://doi.org/10.4028/www.scientific.net/MSF.924.385.
31. D.K. Schroder, *Semiconductor Material and Device Characterization*, 3rd edn. (Wiley, New Jersey, 2006), pp. 135–157.
32. L. Jablonka, L. Riekehr, Z. Zhang, S.L. Zhang, and T. Kubart, *Appl. Phys. Lett.* (2018). https://doi.org/10.1063/1.5011109.
33. R. Pretorius, J.M. Harris, and M.A. Nicolet, *Solid-State Electron.* (1978). https://doi.org/10.1016/0038-1101(78)90335-0.
34. T. Nguyen, H.L. Ho, D.E. Kotecki, and T.D. Nguyen, *J. Appl. Phys.* (1996). https://doi.org/10.1063/1.362667.
35. M.H. Juang, and H.C. Cheng, *Thin Solid Films* (1992). https://doi.org/10.1016/0040-6090(92)90703-E.